Original Article

Pulsatile cerebrospinal fluid dynamics in Chiari I malformation syringomyelia: Predictive value in posterior fossa decompression and insights into the syringogenesis

ABSTRACT

Background: Pathophysiological mechanisms underlying the syringomyelia associated with Chiari I malformation (CM-1) are still not completely understood, and reliable predictors of the outcome of posterior fossa decompression (PFD) are lacking accordingly. The reported prospective case-series study aimed to prove the existence of a pulsatile, biphasic systolic–diastolic cerebrospinal fluid (CSF) dynamics inside the syrinx associated with CM-1 and to assess its predictive value of patients' outcome after PFD. Insights into the syringogenesis are also reported.

Methods: Fourteen patients with symptomatic CM-1 syringomyelia underwent to a preoperative neuroimaging study protocol involving conventional T1/T2 and cardiac-gated cine phase-contrast magnetic resonance imaging sequences. Peak systolic and diastolic velocities were acquired at four regions of interest (ROIs): syrinx, ventral, and dorsal cervical subarachnoid space and foramen magnum region. Data were reported as mean ± standard deviation. After PFD, the patients underwent a scheduled follow-up lasting 3 years. One-way analysis of variance with Bonferroni *Post hoc* test of multiple comparisons was performed *P* was <0.001.

Results: All symptoms but atrophy and spasticity improved. PFD caused a significant velocity changing of each ROI. Syrinx and premedullary cistern velocities were found to be decreased within the 1st month after PFD (<0.001). A caudad and cephalad CSF jet flow was found inside the syrinx during systole and diastole, respectively.

Conclusion: Syrinx and premedullary cistern velocities are related to an early improvement of symptoms in patients with CM-1 syringomyelia who underwent PFD. The existence of a biphasic pulsatile systolic–diastolic CSF pattern inside the syrinx validates the "transmedullary" theory about the syringogenesis.

Keywords: Cerebrospinal fluid circulation, Chiari I malformation, cine magnetic resonance imaging, posterior fossa decompression, syringomyelia

Sabino Luzzi[1,2], Alice Giotta Lucifero[1], Yasmeen Elsawaf[3], Samer K. Elbabaa[3], Mattia Del Maestro[2,4], Gabriele Savioli[4,5], Renato Galzio[6], Cristian Gragnaniello[7]

[1]Department of Clinical-Surgical, Diagnostic and Pediatric Sciences, Neurosurgery Unit, University of Pavia, [2]Department of Surgical Sciences, Neurosurgery Unit, Fondazione IRCCS Policlinico San Matteo, [4]Department of Clinical-Surgical, Diagnostic and Pediatric Sciences, University of Pavia, [5]Department of Emergency, Fondazione IRCCS Policlinico San Matteo, Pavia, [6]Department of Neurosurgery, Maria Cecilia Hospital, Cotignola, Italy, [3]Department of Pediatric Neurosurgery, Leon Pediatric Neuroscience Center of Excellence, Arnold Palmer Hospital for Children, Orlando, Florida, [7]Department of Neurological Surgery, University of Illinois at Chicago, Chicago, IL, USA

Address for correspondence: Dr. Sabino Luzzi, Polo Didattico "Cesare Brusotti", Viale Brambilla, 74-27100, Pavia, Italy.
E-mail: sabino.luzzi@unipv.it

Submitted: 08-Apr-20 **Accepted:** 26-Dec-20
Published: 04-Mar-21

INTRODUCTION

The prevalence of syringomyelia ranges from 40% to 70% in patients with Chiari I malformation (CM-1), and the coexistence of both these conditions makes the decision-making process about the indication for surgery even more difficult.[1,2] The main reasons for this lie in the still debated pathogenesis about the syrinx formation, heterogeneous symptomatology,

Videos Available on: www.jcvjs.com

Access this article online

Website: www.jcvjs.com

Quick Response Code

DOI: 10.4103/jcvjs.JCVJS_42_20

How to cite this article: Luzzi S, Giotta Lucifero A, Elsawaf Y, Elbabaa SK, Del Maestro M, Savioli G, *et al.* Pulsatile cerebrospinal fluid dynamics in Chiari I malformation syringomyelia: Predictive value in posterior fossa decompression and insights into the syringogenesis. J Craniovert Jun Spine 2021;12:15-25.

multiplicity of treatment options, and especially dramatically lack of reliable predictors of outcome on the basis of which to select those patients who will most likely benefit from surgery.[3,4] In fact, most of the previous reported predictors include anamnestic factors focused on the type and duration of symptoms, neurologic or quality of life scales, or also static magnetic resonance imaging (MRI) measurements.[3,5,6] Nevertheless, Chiari I-related syringomyelia is a very complex pathology where most of the theories about its formation, persistence, and progression involve dynamic factors of the cerebrospinal fluid (CSF) circulation, volume changes of the spinal canal and its contents, cardiac-related pulsations, abdominal pressure, along with a reduced volume of the posterior fossa.[7-20] On the other hand, the constant evolution of the MRI techniques and the implementation of CSF velocity-coded sequences have led to the comprehension of the fundamental features of the motion of the CSF along the neuraxis. They also provided a noninvasive qualitative–quantitative evaluation of the morphofunctional characteristics of the syrinx during the cardiac cycle.[21-36] Cine phasecontrast has been among the first motion-sensitive MRI sequence proved to have a reliable role in the prediction of patients' outcomes for several pathologies.[11,13,23,24,37-39] Nevertheless, its predictive value in the evaluation of patients affected by syringomyelia has been largely underestimated.

The aim of this prospective case-series study is first to test the hypothesis of the existence of a biphasic, systolic–diastolic CSF pulsatile pattern inside the syrinx, as a result of a communication between the syrinx and the subarachnoid space and second to assess its predictive value of patients' outcome after posterior fossa decompression (PFD). Some insights into the pathophysiology underlying the syrinx formation and the theories about the hindbrain-related syringomyelia are also reported.

METHODS

The present study, approved by the Internal Institutional Review Board, started in January 2015 and finished in December 2019. Eligible criteria were the following: age ranging between 18 and 70 years old, evidence for Chiari 1 malformation and associated syringomyelia, and scheduled PFD surgery. Patients with previous moderate-to-severe brain injuries, CSF pathologies, previous neurosurgical procedures, chronic obstructive pneumopathy, obstructive sleep apnea syndrome, or thoraco-abdominal masses were excluded from the study. In all the patients, an exhaustive neurological assessment aimed to detect symptoms and signs related to the syrinx and CM-1 was evaluated preoperatively. All the patients underwent T1-T2-weighted spin-echo images of the brain and spine. The preoperative imaging workup was also involved by default retrospective cardiac-gated cine phase-contrast MRI (Magnetom 1.5T MRI Scanner, Siemens Healthineers, Erlangen, Germany, in all of them). Acquisition datasets were as follows: repetition time: 50 ms, echo time: 10 ms, flip angle: 15°, two signals acquisition, 256 × 192 matrix, thickness: 3 mm, velocity encoding: 5 cm/s, and increased to 10 cm/s in case of aliasing. A retrospective cardiac gating technique was used. Cardiac triggering was achieved with finger photoplethysmography. Radio-frequency pulses ranged between 12 and 24 depending on the heart rate, which, in turn, ranged between 50 and 100 bpm. CSF flow data were acquired in mid-sagittal and axial planes.

Cardiac cycle was fractioned in 14 different phases and the highest velocity (peak) was calculated both in systole and diastole for each voxel within each region of interest (ROI) at each of these phases. Acquired images were reviewed in a video loop mode studying the relationships of the cardiac cycle on the motion of the CSF within the subarachnoid space.

Four ROIs were studied in detail, namely the syrinx, cervical ventral, and dorsal subarachnoid space and foramen magnum. The measurements were executed with a DICOM imaging workstation (Osirix DICOM Viewer@, Pixmeo, Bernex, Switzerland).

Craniocaudal length and maximum anterior–posterior (AP) diameter of the syrinx were calculated on the sagittal and axial T2-weighted MRI, respectively. Maximum AP diameter of the ventral and dorsal cervical subarachnoid space (C-SAS) was measured on sagittal and axial T2 MRI at the level of the C4–C5 intervertebral disk. AP diameter of premedullary cistern and cisterna magna was measured at the level of the McRae line. Peak systolic and diastolic velocities were calculated at each ROI and reported as mean ± standard deviation.

All the patients underwent a PFD. Surgeries were executed by the same surgeon (RG) and involved in all cases a wide suboccipital craniectomy, C1 laminectomy, or C1 and C2 depending on cases, dura opening, microneurolysis of the arachnoid bends at the level of foramen of Magendie, and duraplasty with a xenogeneic bovine pericardium dural substitute (Tutopatch, SIAD Healthcare S.p.a., Assago, Milano, Italy). The scheduled follow-up involved a postoperative – within 72 h – neurological evaluation, along with the same neuroimaging protocol performed preoperatively. The same clinicoradiological evaluations were executed at the 1st, 2nd, 3rd, and 6th month and 1st, 2nd, and 3rd year after the PFD. Statistical analysis was carried out by means of a commercially available software (SPSS Statistics for Windows, version x. 0, SPSS Inc., Chicago, IL, USA).

One-way analysis of variance (ANOVA) was performed for each parameter. Significant results in the ANOVA model were further investigated with Bonferroni *Post hoc* test of multiple comparisons. *P* was set as ≤0.001. The results were reported based on the Strengthening the Reporting of Observational Study in Epidemiology statement.[40]

RESULTS

Demographic data

Fourteen patients were enrolled. Patients' ages ranged between 17 and 51 years, with an average age of 30.5 years. The male/female ratio was 0.7.

Symptoms and spinal cord metameric involvement

Data about preoperative symptoms are reported in Graph 1. Headache, dissociated sensory loss, lower cranial nerve dysfunction, and weakness were most frequent. C2–C5 metameres were most frequently involved [Graph 2]. Headache immediately disappeared after surgery, whereas a full recovery from dysesthetic pain, weakness, and dissociated sensory loss was seen in all the treated patients within 6 months. Conversely, atrophy and spasticity were almost unaffected by surgery. The overall trend of symptoms and clinical signs is reported in Graph 3.

Magnetic resonance imaging and cine phase-contrast magnetic resonance imaging data

Overall data about the ROI measurements are reported in Table 1.

Syrinx

All the syrinx parameters decreased after surgery (<0.001) [Graphs 4-6]. Bonferroni multiple comparisons test showed that the length and AP diameter decreased at 1st year and 1st month, respectively, whereas systolic and diastolic peak velocity declined at postoperative and 2nd-month follow-up, respectively [Table 2].

Ventral (cervical subarachnoid space)

AP diameter increases immediately after surgery (<0.001) [Graph 7]. Peak systolic and diastolic velocities significantly decreased at 3rd-and 6th-month, respectively [Graph 8 and Table 3].

Dorsal (cervical subarachnoid space)

AP diameter increased starting from the 3rd month after surgery [Graph 9]. Here, the systolic velocity diminished very earlier than the diastolic one [Graph 10 and Table 4].

Foramen magnum region

Premedullary cistern showed a significant enlargement 3 months after surgery [Graph 11], whereas cisterna magna appeared effectively increased by surgery [Graph 12].

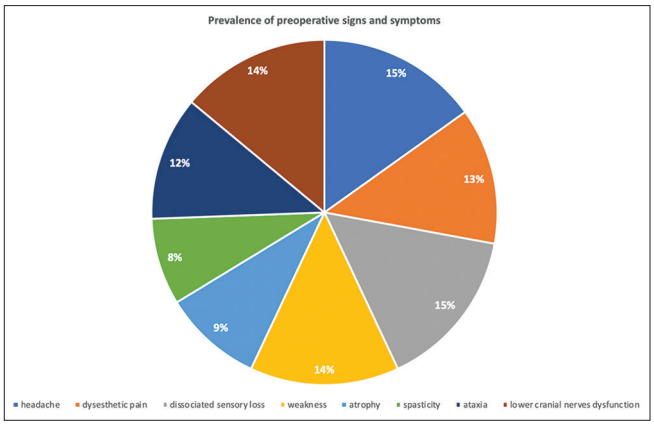

Graph 1: Prevalence of preoperative signs and symptoms

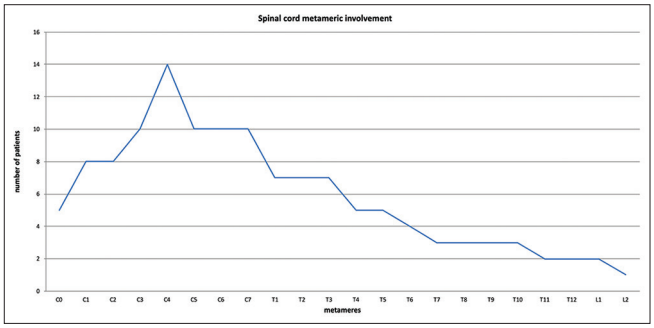

Graph 2: Spinal cord metameric involvment

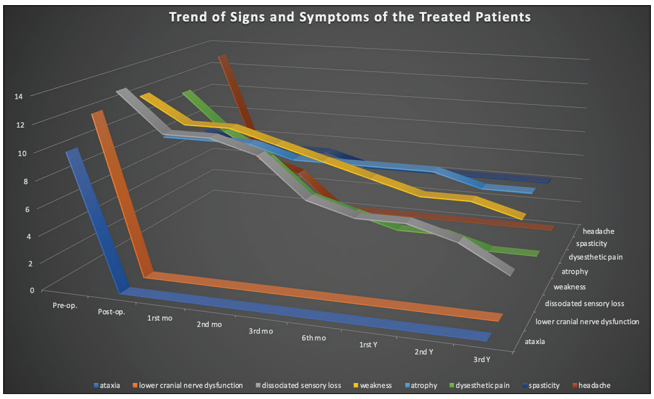

Graph 3: Trend of signs and symptoms of treated patients

Diastolic peak velocity dramatically decreased immediately after surgery, and systolic velocity reduced at the 1st month [Graph 13]. Table 5 summarizes the ANOVA and Bonferroni multiple comparisons tests about the foramen magnum region.

Illustrative cases

Case no. 1

A 45-year-old female with occasional history of headache exacerbated by cough, underwent a laparoscopic cholecystectomy for a gallstone disease. Two weeks later, she started to suffer from a severe ataxia, dysphagia, and dysesthetic

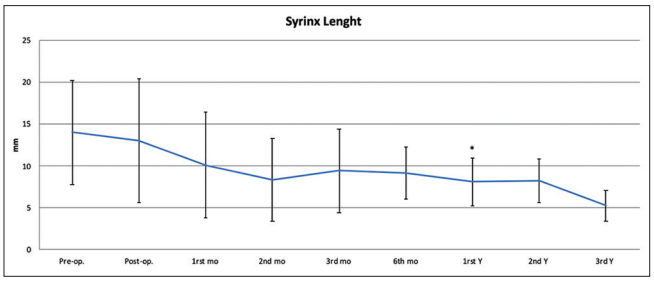

Graph 4: Syrinx lenght

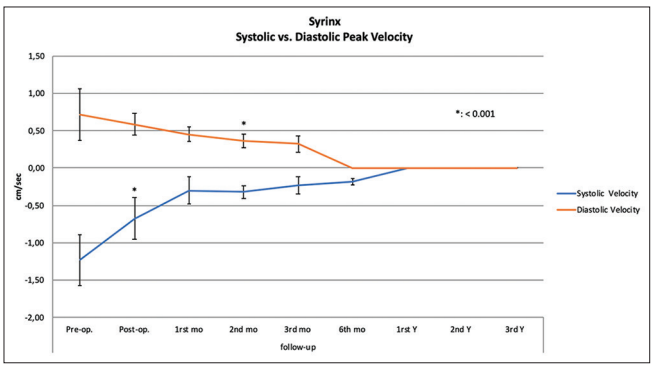

Graph 6: Syrinx systolic versus diastolic peak velocy

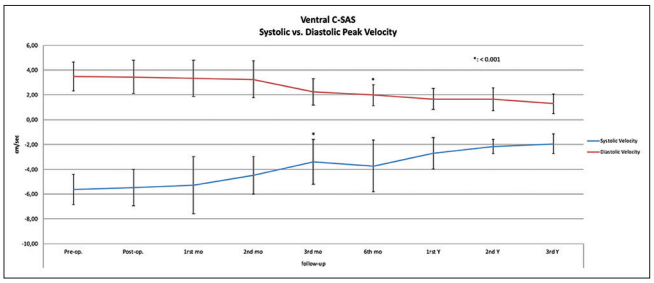

Graph 8: Ventral cervical subarachnoid space syastolic versus diastolic peak velocity

pain and underwent a brain MRI, later completed with a spinal MRI study. A CM-1 associated with a holocord syringomyelia was found [Figure 1a-c]. Cine phase-contrast MRI showed, during systole, the cerebellar tonsils moving downward and acting as a piston on the trapped spinal CSF pathways. Concomitantly, the syrinx dilated in a caudad direction showed a jet CSF flow toward more caudal metameres [Figure 1d]. Conversely, during diastole, the signal inside the syrinx became hypointense as a consequence of the cranial direction of the CSF flow, and the upper part of the syrinx re-expanded. The patient underwent a PFD. At the 1st month of evaluation, the symptoms disappeared almost completely, and the cine MRI revealed a dramatic reduction of the caudad flow inside the syrinx during systole [Figure 1e and Video 1].

Case no. 2

A 42-year-old female underwent a brain MRI because she was suffering from a drug-resistant headache with a dissociated

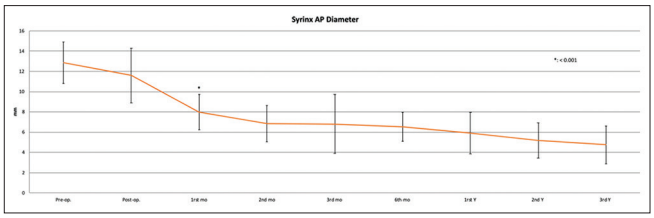

Graph 5: Syrinx anterior–posterior diameter

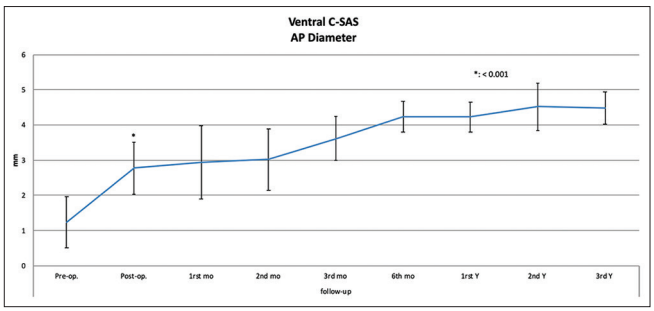

Graph 7: Ventral cervical subarachnoid space anterior–posterior diameter

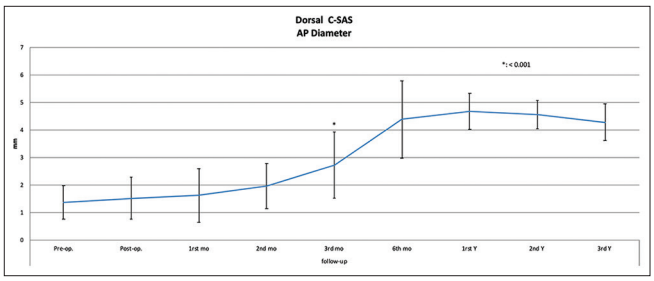

Graph 9: Dorsal cervical subarachnoid space anterior–posterior diameter

sensory loss in the arms. A CM-1 was found, with a C2-T1 syrinx [Figure 2a and b]. Preoperative cine MRI clearly showed a caudad hyperintense signal inside the syrinx during systole [Figure 2c]. During diastole, a tenuous hypointense signal was visible inside the syrinx as a consequence of the cephalad CSF flow [Figure 2d]. The patient was operated on by means of a PFD. The postoperative cine MRI was performed 48 h after surgery revealed a significant attenuation of the systolic signal inside the syrinx [Figure 2e]. The same signal was found to be almost disappeared at the 1st-month evaluation [Figure 2f and Video 2].

Case no. 3

A 37-year-old male with a severe spinal deformity was diagnosed with a CM-1 and a concomitant C2–C7 syringomyelia [Figure 3a]. The patient reported severe headach and a slow but progressive dissociated sensory loss in the arms, especially during the Valsalva maneuver and cough. Cine MRI revealed a caudal CSF jet flow inside the syrinx during systole [Figure 3b and Video 3]. After PFD, the sagittal extension and the AP diameter of the syrinx collapsed already in the early postoperative evaluation [Figure 3c]. Cine MRI performed at the 2nd month

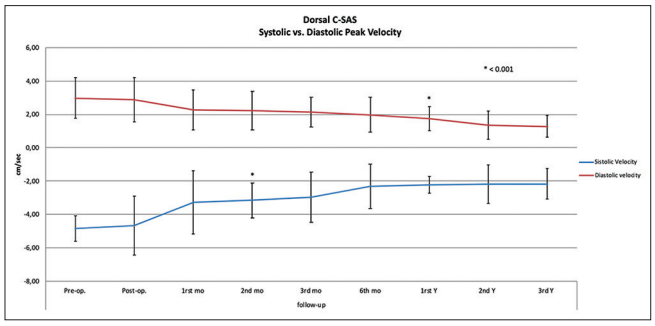

Graph 10: Dorsal cervical subarachnoid space systolic versus diastolic peak velocity

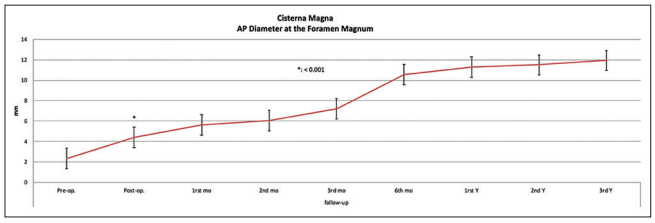

Graph 12: Cisterna magna anterior–posterior diameter at the foramen magnum

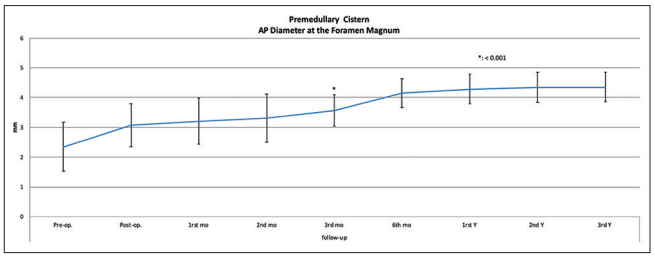

Graph 11: Premedullary cistern anterior–posterior diameter at foramen magnum

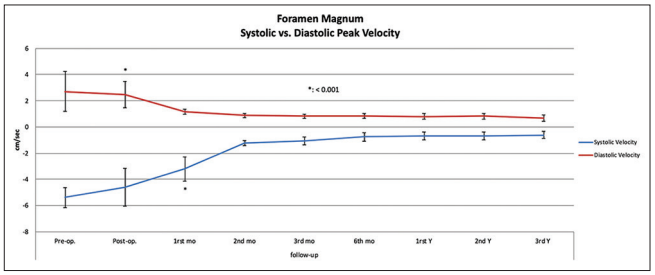

Graph 13: Foramen magnum systolic versus diastolic peak velocity

showed the disappearance of the systolic signal inside the syrinx [Figure 3d and Video 4]. The patient recovered almost completely from his symptoms within 3 months.

DISCUSSION

The natural history of the hindbrain-related syringomyelia is characterized by a stepwise and severe myelopathy causing a progressive neurological deterioration mainly characterized by the occurrence of paralysis, sensory loss, and drug-resistant chronic pain.[41,42] The already controversial landscape related to the management of syringomyelia associated with Chari I malformation is furtherly complicated by the lack of reliable predictors of outcome based on which to better select those patients who could benefit from the PFD. In the past two decades, the advent and implementation of the velocity-coded cine phase-contrast MRI sequences in the routine clinical practice have allowed to shift from a static to a dynamic conception of the CSF pathologies at large, dramatically changing the approach to these illnesses. Cine MRI has also led to new insights into the pathophysiology of the CSF circulation.[23,24,11,13,37-39] A further valuable strength of this technique lies undoubtedly in its noninvasiveness, which furtherly justifies its wide employment. The employment of the cine-phase contrast MRI in CM-1 patients with syringomyelia is not a novelty. Nevertheless, almost the totality of the reported studies focused on parameters different from the direct measurement of the velocities inside the syrinx.[43-52] The results of the present study allow to confirm the existence of a systolic–diastolic pulsatile pattern inside the syrinx, which can be measured preoperatively by means of cine phase-contrast MRI, thus achieving quantitative and qualitative paramount information about the syrinx itself. According to the reported data, the preoperative average syrinx velocity was 1.23 ± 0.34 and 0.72 ± 0.35 cm/s for the systolic and diastolic one, respectively. Similar results have been reported by Honey *et al*.[53-55] After the PFD, we found a significant decrease of the peak systolic velocity already in the immediate postoperative evaluation. The reduction of diastolic velocity resulted significant starting from the 2nd-month follow-up, these data suggesting a later normalization of this parameter compared with the systolic velocity. The disappearance of the systolic–diastolic pattern inside the syrinx follows mainly the trend of the recovery from ataxia, lower cranial nerve dysfunction, dysesthetic pain, and headache. At the level of the foramen magnum region, average peak systolic velocity of the premedullary cistern also decreased immediately after surgery, allowing to identify this parameter as a positive predictor of outcome. Furthermore, the increase of the AP diameter of the premedullary cistern became significant starting from 3 months after surgery, namely much more belatedly than the normalization of the systolic CSF velocity. In contrast, the normalization of the velocities in correspondence of the ventral C-SAS occurred at the 3rd- and 6th month follow-up indicated a poor correlation between the C-SAS velocities and the recovery from symptoms. Similar data regraded the dorsal C-SAS.

The findings of the present study also lead to important considerations about the main theories explaining the formation and progression of the syringomyelia in patients with CM-1.

Briefly, the seminal "pressure dissociation" or "slosh" theory of syrinx progression by Williams,[15,56-58] later revised by Oldfield *et al*. and Heiss *et al*.,[12,13] involved that the presence of a CSF flow obstruction at the craniovertebral junction causes a pressure dissociation between the cranial and spinal subarachnoid spaces by means of a "ball valve mechanism." CSF would pass the area of obstruction during coughing, sneezing, or Valsalva but would be unable to flow back once the spinal pressure had normalized. In the Williams theory,

Table 1: Overall Data about the ROIs Measurements

ROI and Parameter	Pre-op.	Post-op.	1rst mo	2nd mo	3rd mo	6th mo	1rst Y	2nd Y	3rd Y
SYRINX									
Length (cm)									
AVERAGE	14,01	13,06	10,11	8,32	9,41	9,19	8,12	8,21	5,27
SD	6,22	7,39	6,29	4,94	4,98	3,13	2,86	2,61	1,83
AP diameter (mm)									
AVERAGE	12,85	11,60	7,98	6,82	6,80	6,53	5,92	5,18	4,76
SD	2,05	2,70	1,75	1,79	2,90	1,41	2,05	1,74	1,87
Sys Vel. (cm/sec.)									
AVERAGE	1,23	0,67	0,30	0,32	0,23	0,18	ND	ND	ND
SD	0,34	0,28	0,18	0,09	0,12	0,04	ND	ND	ND
Dias Vel. (cm/sec.)									
AVERAGE	0,72	0,58	0,45	0,36	0,32	ND	ND	ND	ND
SD	0,35	0,15	0,10	0,09	0,11	ND	ND	ND	ND
VENTRAL C-SAS									
AP diameter (mm)									
AVERAGE	1,23	2,78	2,94	3,02	3,62	4,24	4,23	4,52	4,48
SD	0,72	0,74	1,04	0,87	0,63	0,43	0,42	0,67	0,46
Sys Vel. (cm/sec.)									
AVERAGE	5,63	5,47	5,28	4,48	3,38	3,73	2,68	2,16	1,94
SD	1,20	1,45	2,32	1,50	1,81	2,09	1,27	0,57	0,78
Dias Vel. (cm/sec.)									
AVERAGE	3,48	3,45	3,35	3,26	2,24	1,98	1,67	1,65	1,28
SD	1,18	1,34	1,46	1,47	1,08	0,84	0,83	0,93	0,78
DORSAL C-SAS									
AP diameter (mm)									
AVERAGE	1,36	1,52	1,62	1,96	2,72	4,38	4,67	4,56	4,27
SD	0,60	0,77	0,97	0,82	1,21	1,41	0,65	0,51	0,67
Sys Vel. (cm/sec.)									
AVERAGE	4,84	4,68	3,27	3,16	2,98	2,32	2,24	2,18	2,16
SD	0,77	1,76	1,90	1,06	1,50	1,35	0,50	1,16	0,91
Dias Vel. (cm/sec.)									
AVERAGE	2,98	2,87	2,25	2,23	2,14	1,98	1,76	1,37	1,28
SD	1,22	1,34	1,20	1,15	0,88	1,05	0,73	0,85	0,64
FORAMEN MAGNUM REGION									
Premedullary Cistern AP Diameter (mm)									
AVERAGE	2,35	3,07	3,21	3,30	3,57	4,14	4,28	4,35	4,35
SD	0,81	0,72	0,78	0,81	0,53	0,48	0,49	0,50	0,50
Cisterna Magna AP Diameter (mm)									
AVERAGE	2,36	4,42	5,64	6,07	7,21	10,57	11,29	11,50	11,93
SD	0,44	0,68	0,82	0,66	0,87	1,38	1,72	1,36	2,03
Sys Vel. (cm/sec.)									
AVERAGE	5,39	4,62	3,21	1,22	1,08	0,75	0,70	0,68	0,62
SD	0,78	1,43	0,92	0,18	0,30	0,32	0,30	0,29	0,28
Dias Vel. (cm/sec.)									
AVERAGE	2,71	2,46	1,16	0,87	0,83	0,82	0,81	0,81	0,66
SD	1,52	1,00	0,20	0,15	0,17	0,19	0,22	0,23	0,23

AP: anterior-posterior; C-SAS: cervical subarachnoid space; Dias: diastolic velocity, mo: month; ND: not detectable; ROI: Region of Interest; SD: standard deviation; Sys: systolic velocity; Y: year.

Table 2: Summary of ANOVA and Bonferroni multiple comparisons tests of the Syrinx Parameters

Parameter	*P*						
	ANOVA	Bonferroni Multiple Comparisons					
	Overall Follow-Up	Pre-op vs. Post-op	Pre-op vs. 1rst mo	Pre-op vs. 2nd mo	Pre-op vs. 3rd mo	Pre-op vs. 6th mo	Pre-op vs. 1rts Y
Length	<0.001	0.717	0.265	0.012	0.040	0.015	<0.001
AP diameter	<0.001	0.179	<0.001	nc	nc	nc	nc
Systolic Velocity	<0.001	<0.001	nc	nc	nc	nc	nc
Diastolic Velocity	<0.001	0.187	0.009	<0.001	nc	nc	nc

AP: anterior-posterior; mo: month; Y: year; nc: not calculated

Table 3: Summary of ANOVA and Bonferroni multiple comparisons tests of the Ventral C-SAS

Parameter	*P*						
	ANOVA	Bonferroni Multiple Comparisons					
	Overall Follow-Up	Pre-op vs. Post-op	Pre-op vs. 1rst mo	Pre-op vs. 2nd mo	Pre-op vs. 3rd mo	Pre-op vs. 6th mo	Pre-op vs. 1rts Y
AP diameter	<0.001	0.001	nc	nc	nc	nc	nc
Systolic Velocity	<0.001	0,754	0,801	0,035	<0.001	nc	nc
Diastolic Velocity	<0.001	0,948	0,790	0,653	0,007	<0.001	nc

AP: anterior-posterior; C-SAS: cervical subarachnoid space; mo: month; nc: not calculated; Y: year.

Table 4: Summary of ANOVA and Bonferroni multiple comparisons tests of the Dorsal C-SAS

Parameter	*P*						
	ANOVA	Bonferroni Multiple Comparisons					
	Overall Follow-Up	Pre-op vs. Post-op	Pre-op vs. 1rst mo	Pre-op vs. 2nd mo	Pre-op vs. 3rd mo	Pre-op vs. 6th mo	Pre-op vs. 1rst Y
AP diameter	<0.001	0,830	0,123	0,104	0,046	0,027	<0.001
Systolic Velocity	<0.001	0,757	0,008	<0.001	nc	nc	nc
Diastolic Velocity	<0.001	0,830	0,123	0,104	0,046	0,027	<0.001

AP: anterior-posterior; C-SAS: cervical subarachnoid space; mo: month; nc: not calculated; Y: year.

Table 5: Summary of ANOVA and Bonferroni multiple comparisons tests of the Foramen Magnum Region

Parameter		*P*				
		ANOVA	Bonferroni Multiple Comparisons			
		Overall Follow-Up	Pre-op vs. Post-op	Pre-op vs. 1rst mo	Pre-op vs. 2nd mo	Pre-op vs. 3rd mo
Premedullary Cistern	AP diameter	<0.001	0,019	0,008	0,008	<0.001
Cisterna Magna	AP diameter	<0.001	<0.001	nc	nc	nc
Foramen Magnum	Systolic Velocity	<0.001	0,090	<0.001	nc	nc
	Diastolic Velocity	<0.001	<0.001	nc	nc	Nc

AP: anterior-posterior; mo: month; nc: not calculated; Y: year.

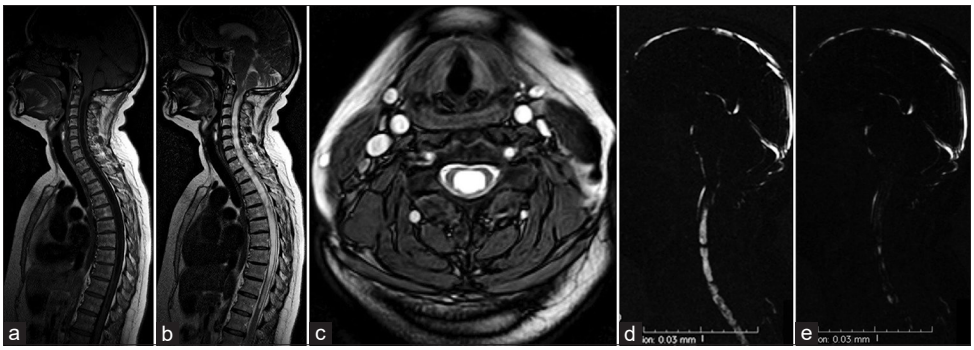

Figure 1: Sagittal T1- (a) and T2-weighted magnetic resonance imaging (b) of the brain and spine, and axial T2-weighted magnetic resonance imaging (c) (C4–C5 intervertebral disk) showing a Chiari I malformation with a holocord syringomyelia. (d) Preoperative cine phase-contrast magnetic resonance imaging during systole revealing the cerebellar tonsils moving downward, the dilation of the syrinx synchronous with the systole, and a cerebrospinal fluid jet flow inside the syrinx. (e) Cine magnetic resonance imaging performed 1 month after posterior fossa decompression documenting a significant systolic reduction of flow inside the syrinx

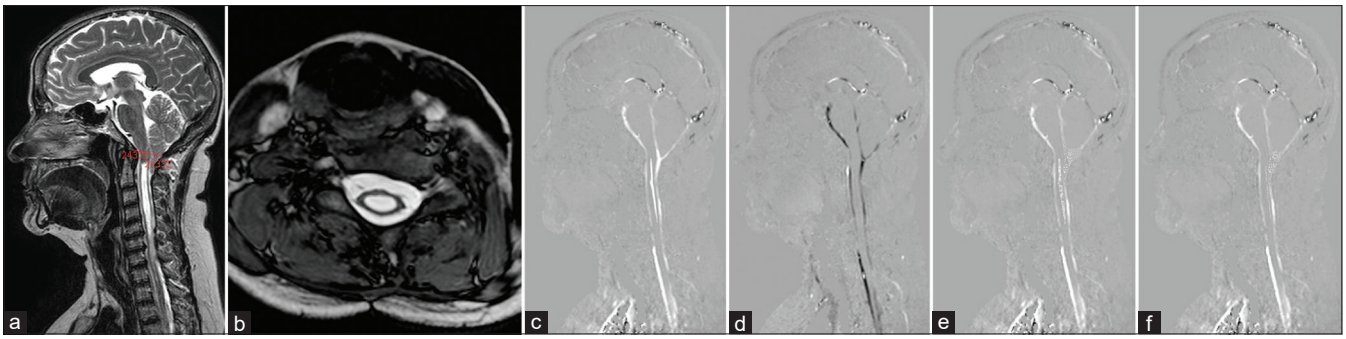

Figure 2: Sagittal (a) and axial (b) T2-weighted magnetic resonance imaging showing a Chiari I malformation with a C2–T1 syrinx. (c) Preoperative cine magnetic resonance imaging revealing a caudad hyperintense signal inside the syrinx cavity during systole. (d) Preoperative cine magnetic resonance imaging during diastole showing a tenuous hypointense signal due to the cephalad cerebrospinal fluid flow. (e and f) Postoperative cine magnetic resonance imaging performed at the early postoperative and 1st-month follow-up, respectively, showing a progressive disappearance of the systolic signal inside the syrinx

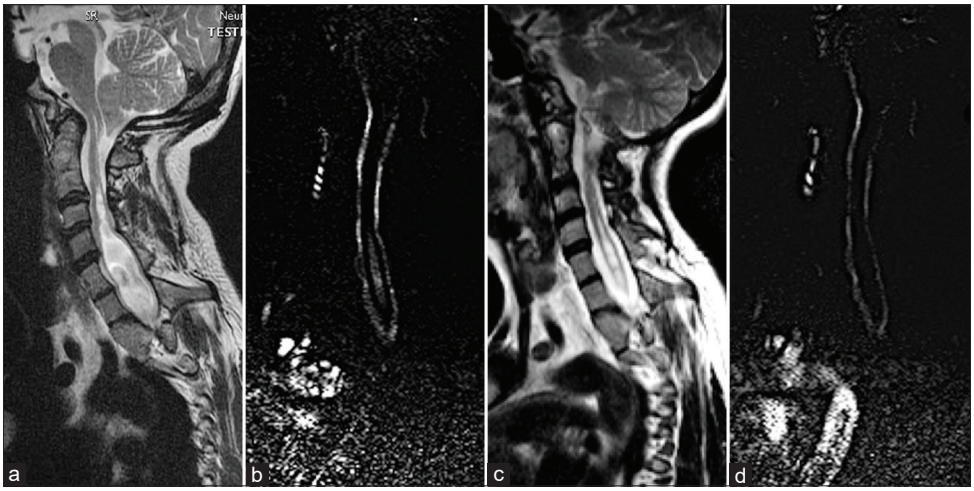

Figure 3: (a) Sagittal T2-weighted magnetic resonance imaging documenting a C2–C7 syrinx in a patient with a severe spinal deformity associated with a Chari I malformation. (b) Preoperative cine magnetic resonance imaging demonstrating the existence of a caudal cerebrospinal fluid jet flow during systole, mainly involving the most caudal part of the syrinx. (c) Postoperative sagittal T2-weighted magnetic resonance imaging performed at the 2nd-month follow-up and revealing a significant collapse of the syrinx. (d) Postoperative Cine magnetic resonance imaging confirming the complete disappearance of the systolic signal inside the syrinx

the intracranial pressure would then be normalized by the CSF flowing through the obex into the central canal, ultimately leading to the syrinx formation.[56,57] Increasing abdominal pressure is transmitted to the epidural spinal veins producing an ascending venous pressure wave from the spinal subarachnoid space through the foramen magnum. Due to the obstruction at the level of craniocervical junction, the pressure wave ascends to the spinal axis, expanding the syrinx.[56,57] Oldfield *et al*. and Heiss *et al*. proved that in the presence of an obstruction of the foramen magnum and a "piston effect" by the cerebellar tonsils on the spinal subarachnoid space, increasing of abdominal pressure is transmitted to the spinal cord through the Virchow–Robin perivascular spaces.[12,13] They also demonstrated that the propelling force at the base of this "transmedullary" CSF flow is the heartbeat, with systole and diastole leading to a self-maintaining mechanism. Indeed, a CSF flow through the Virchow–Robin perivascular spaces associated with the genesis of syringomyelia was described several years before by Ball and Dayan.[7]

Rai and Rai reported in 2015 their valuable alternative hypothesis about the Chiari malformation-associated syringogenesis, namely the "volume change" theory.[16] This theory is based on the CSF flow dynamics at the level of the posterior fossa and the subsequent changes in volume of the spinal canal and its content during flexion and extension of the head, leading to the syrinx formation as a compensatory mechanism.

The "volume change" theory constitutes the rationale for Goel's technique, namely stand-alone C1–C2 fixation. This because the instability of the atlantoaxial complex has been reported to be the cause of Chiari 1 malformation, syringomyelia, and basilar invagination.[59-62] Based on this evidence, syringomyelia secondary to Chiari malformation

ought to be treated with stabilization of the atlantoaxial joint, with no need for PFD with or without intradural manipulation.[63-68]

In our study, the finding of a clear systolic pattern of the injection of the syrinx by a CSF jet flow which is synchronous with the heartbeat, as reported in the illustrative case, supports the Oldfield and Heiss "transmedullary" theory.

This concept is furtherly reinforced by the fact that, according to these observations, CSF systolic velocity inside the syrinx decreases immediately after surgery.

From a technical standpoint, the adjustment of the velocity encoding in case of aliasing is the key to avoid artifacts during acquisition of the dynamic CSF study.

Limitations of the study

Our study has some important limitations which ought to be mentioned. First, the number of the patients is limited and series by far wider are necessary to draw a definitive conclusion and to validate the proposed neuroimaging study algorithm as the approach of choice in these patients. Second, the search for a systolic–diastolic CSF flow pattern is often difficult to achieve during cine phase-contrast MRI, and the technique is affected by a not-negligible risk of false positives and negatives. Artifacts coming from a limited velocity encoding or aspects as prospective versus retrospective cardiac gating are further technical aspects making difference. Third, the reported study did not involve a control group, being basically an observational case series study. Randomized trials are necessary to achieve definitive conclusions.

CONCLUSION

A biphasic systolic–diastolic CSF pulsatile pattern, detected with cine phase-contrast MRI, can be documented in a large part of the patients diagnosed with syringomyelia associated with Chari I malformation.

PFD causes an early decrease of the velocities inside the syrinx and at the level of the foramen magnum. These velocities are predictors of positive outcome for an early recovery from headache, dysesthetic pain, weakness, lower cranial nerve dysfunction, and dissociated sensory loss.

The evidence of a pulsatile CSF flow pattern inside the syrinx supports the Oldfield and Heiss "transmedullary" theory about the formation and progression of the syrinx.

Further studies are necessary the definitively validate these data.

Financial support and sponsorship

Nil.

Conflicts of interest

There are no conflicts of interest.

REFERENCES

1. Kahn EN, Muraszko KM, Maher CO. Prevalence of Chiari I malformation and syringomyelia. Neurosurg Clin N Am 2015;26:501-7.
2. Langridge B, Phillips E, Choi D. Chiari malformation Type 1: A systematic review of natural history and conservative management. World Neurosurg 2017;104:213-9.
3. Atchley TJ, Alford EN, Rocque BG. Systematic review and meta-analysis of imaging characteristics in Chiari I malformation: Does anything really matter? Childs Nerv Syst 2020;36:525-34.
4. Greenberg JK, Milner E, Yarbrough CK, Lipsey K, Piccirillo JF, Smyth MD, *et al*. Outcome methods used in clinical studies of Chiari malformation Type I: A systematic review. J Neurosurg 2015;122:262-72.
5. Arora P, Behari S, Banerji D, Chhabra DK, Jain VK. Factors influencing the outcome in symptomatic Chiari I malformation. Neurol India 2004;52:470-4.
6. Attenello FJ, McGirt MJ, Gathinji M, Datoo G, Atiba A, Weingart J, *et al*. Outcome of Chiari-associated syringomyelia after hindbrain decompression in children: Analysis of 49 consecutive cases. Neurosurgery 2008;62:1307-13.
7. Ball MJ, Dayan AD. Pathogenesis of syringomyelia. Lancet 1972;2:799-801.
8. du Boulay G, Shah SH, Currie JC, Logue V. The mechanism of hydromyelia in Chiari Type 1 malformations. Br J Radiol 1974;47:579-87.
9. Gardner WJ. Hydrodynamic factors in Dandy-Walker and Arnold-Chiari malformations. Childs Brain 1977;3:200-12.
10. Gardner WJ, Angel J. The mechanism of syringomyelia and its surgical correction. Clin Neurosurg 1958;6:131-40.
11. Haughton VM, Korosec FR, Medow JE, Dolar MT, Iskandar BJ. Peak systolic and diastolic CSF velocity in the foramen magnum in adult patients with Chiari I malformations and in normal control participants. AJNR Am J Neuroradiol 2003;24:169-76.
12. Heiss JD, Patronas N, DeVroom HL, Shawker T, Ennis R, Kammerer W, *et al*. Elucidating the pathophysiology of syringomyelia. J Neurosurg 1999;91:553-62.
13. Oldfield EH, Muraszko K, Shawker TH, Patronas NJ. Pathophysiology of syringomyelia associated with Chiari I malformation of the cerebellar tonsils. Implications for diagnosis and treatment. J Neurosurg 1994;80:3-15.
14. Rusbridge C, Greitz D, Iskandar BJ. Syringomyelia: Current concepts in pathogenesis, diagnosis, and treatment. J Vet Intern Med 2006;20:469-79.
15. Williams B. The distending force in the production of "communicating syringomyelia". Lancet 1969;2:189-93.
16. Rai SK, Rai PS. Volume change theory for syringomyelia: A new perspective. Asian J Neurosurg 2015;10:245-51.
17. Goel A. Basilar invagination, syringomyelia and Chiari formation and their relationship with atlantoaxial instability. Neurol India 2018;66:940-2.
18. Goel A. Atlantoaxial instability and Chiari malformation-response. J Neurosurg Spine 2015;22:560.
19. Goel A. Basilar invagination, Chiari malformation, syringomyelia: A review. Neurol India 2009;57:235-46.
20. Luzzi S, Lucifero AG, Pacilli M, Tartaglia N, Ambrosi A. Hindbrain□related syringomyelia and raised intra□abdominal pressure: implications for safety of laparoscopic and robotic surgery. Ann Ital Chir 2020;9:S0003469X20032832.

21. Armonda RA, Citrin CM, Foley KT, Ellenbogen RG. Quantitative cine-mode magnetic resonance imaging of Chiari I malformations: An analysis of cerebrospinal fluid dynamics. Neurosurgery 1994;35:214-23.
22. Bhadelia RA, Bogdan AR, Kaplan RF, Wolpert SM. Cerebrospinal fluid pulsation amplitude and its quantitative relationship to cerebral blood flow pulsations: A phase-contrast MR flow imaging study. Neuroradiology 1997;39:258-64.
23. Bhadelia RA, Bogdan AR, Wolpert SM, Lev S, Appignani BA, Heilman CB. Cerebrospinal fluid flow waveforms: Analysis in patients with Chiari I malformation by means of gated phase-contrast MR imaging velocity measurements. Radiology 1995;196:195-202.
24. Brugières P, Idy-Peretti I, Iffenecker C, Parker F, Jolivet O, Hurth M, *et al*. CSF flow measurement in syringomyelia. AJNR Am J Neuroradiol 2000;21:1785-92.
25. Du Boulay G, O'Connell J, Currie J, Bostick T, Verity P. Further investigations on pulsatile movements in the cerebrospinal fluid pathways. Acta Radiol Diagn (Stockh) 1972;13:496-523.
26. Enzmann DR, Pelc NJ. Brain motion: Measurement with phase-contrast MR imaging. Radiology 1992;185:653-60.
27. Enzmann DR, Pelc NJ. Cerebrospinal fluid flow measured by phase-contrast cine MR. AJNR Am J Neuroradiol 1993;14:1301-7.
28. Enzmann DR, Pelc NJ. Normal flow patterns of intracranial and spinal cerebrospinal fluid defined with phase-contrast cine MR imaging. Radiology 1991;178:467-74.
29. Greitz D, Wirestam R, Franck A, Nordell B, Thomsen C, Stahlberg F. Pulsatile brain movement and associated hydrodynamics studied by magnetic resonance phase imaging. The Monro-Kellie doctrine revisited. Neuroradiology 1992;34:370-80.
30. Henry-Feugeas MC, Idy-Peretti I, Blanchet B, Hassine D, Zannoli G, Schouman-Claeys E. Temporal and spatial assessment of normal cerebrospinal fluid dynamics with MR imaging. Magn Reson Imaging 1993;11:1107-18.
31. Levy LM, Di Chiro G. MR phase imaging and cerebrospinal fluid flow in the head and spine. Neuroradiology 1990;32:399-406.
32. Nitz WR, Bradley WG Jr., Watanabe AS, Lee RR, Burgoyne B, O'Sullivan RM, *et al*. Flow dynamics of cerebrospinal fluid: Assessment with phase-contrast velocity MR imaging performed with retrospective cardiac gating. Radiology 1992;183:395-405.
33. Quencer RM, Post MJ, Hinks RS. Cine MR in the evaluation of normal and abnormal CSF flow: Intracranial and intraspinal studies. Neuroradiology 1990;32:371-91.
34. Schroth G, Klose U. Cerebrospinal fluid flow. I. Physiology of cardiac-related pulsation. Neuroradiology 1992;35:1-9.
35. Firmin DN, Nayler GL, Klipstein RH, Underwood SR, Rees RS, Longmore DB. *In vivo* validation of MR velocity imaging. J Comput Assist Tomogr 1987;11:751-6.
36. Wang DD, Martin KW, Auguste KI, Sun PP. Fast dynamic imaging technique to identify obstructive lesions in the CSF space: Report of 2 cases. J Neurosurg Pediatr 2015;15:519-23.
37. Armonda RA, Citrin CM, Foley KT, Ellenbogen RG. Quantitative cine-mode magnetic resonance imaging of Chiari I malformations: An analysis of cerebrospinal fluid dynamics. Neurosurgery 1994;35:214-24.
38. Terae S, Miyasaka K, Abe S, Abe H, Tashiro K. Increased pulsatile movement of the hindbrain in syringomyelia associated with the Chiari malformation: Cine-MRI with presaturation bolus tracking. Neuroradiology 1994;36:125-9.
39. Wolpert SM, Bhadelia RA, Bogdan AR, Cohen AR. Chiari I malformations: Assessment with phase-contrast velocity MR. AJNR Am J Neuroradiol 1994;15:1299-308.
40. von Elm E, Altman DG, Egger M, Pocock SJ, Gøtzsche PC, Vandenbroucke JP, *et al*. The Strengthening the Reporting of Observational Studies in Epidemiology (STROBE) statement: Guidelines for reporting observational studies. Lancet 2007;370:1453-7.
41. Boman K, Iivanainen M. Prognosis of syringomyelia. Acta Neurol Scand 1967;43:61-8.
42. Singhal A, Roberts BT, Steinbok P, Cochrane D, Byrne AT, Kerr JM. Natural history of untreated syringomyelia in pediatric patients. Neurosurg Focus 2011;31:E13.
43. Gottschalk A, Schmitz B, Mauer UM, Bornstedt A, Steinhoff S, Danz B, *et al*. Dynamic visualization of arachnoid adhesions in a patient with idiopathic syringomyelia using high-resolution cine magnetic resonance imaging at 3T. J Magn Reson Imaging 2010;32:218-22.
44. Zhu Z, Sha S, Chu WC, Yan H, Xie D, Liu Z, *et al*. Comparison of the scoliosis curve patterns and MRI syrinx cord characteristics of idiopathic syringomyelia versus Chiari I malformation. Eur Spine J 2016;25:517-25.
45. Wang CS, Wang X, Fu CH, Wei LQ, Zhou DQ, Lin JK. Analysis of cerebrospinal fluid flow dynamics and morphology in Chiari I malformation with cine phase-contrast magnetic resonance imaging. Acta Neurochir (Wien) 2014;156:707-13.
46. Wang Y, Xie J, Zhao Z, Zhang Y, Li T, Si Y. Changes in CSF flow after one-stage posterior vertebral column resection in scoliosis patients with syringomyelia and Chiari malformation Type I. J Neurosurg Spine 2013;18:456-64.
47. Clarke EC, Stoodley MA, Bilston LE. Changes in temporal flow characteristics of CSF in Chiari malformation Type I with and without syringomyelia: Implications for theory of syrinx development. J Neurosurg 2013;118:1135-40.
48. Chang HS, Nagai A, Oya S, Matsui T. Dorsal spinal arachnoid web diagnosed with the quantitative measurement of cerebrospinal fluid flow on magnetic resonance imaging. J Neurosurg Spine 2014;20:227-33.
49. Leung V, Magnussen JS, Stoodley MA, Bilston LE. Cerebellar and hindbrain motion in Chiari malformation with and without syringomyelia. J Neurosurg Spine 2016;24:546-55.
50. Bunck AC, Kroeger JR, Juettner A, Brentrup A, Fiedler B, Crelier GR, *et al*. Magnetic resonance 4D flow analysis of cerebrospinal fluid dynamics in Chiari I malformation with and without syringomyelia. Eur Radiol 2012;22:1860-70.
51. Strahle J, Muraszko KM, Kapurch J, Bapuraj JR, Garton HJ, Maher CO. Chiari malformation Type I and syrinx in children undergoing magnetic resonance imaging. J Neurosurg Pediatr 2011;8:205-13.
52. Taylor DG, Chatrath A, Mastorakos P, Paisan G, Chen CJ, Buell TJ, Jane JA. Cerebrospinal fluid area and syringogenesis in Chiari malformation type I. J Neurosurg 2020;21:1-6. doi: 10.3171/2019.11.JNS191439.
53. Honey CM, Martin KW, Heran MK. Syringomyelia fluid dynamics and cord motion revealed by serendipitous null point artifacts during cine MRI. AJNR Am J Neuroradiol 2017;38:1845-7.
54. Park CH, Chung TS, Kim DJ, Suh SH, Chung WS, Cho YE. Evaluation of intrasyrinx fluid motion by spatial modulation of magnetization-magnetic resonance imaging in syringomyelia with long-term follow-up: A predictor of postoperative prognosis? J Comput Assist Tomogr 2008;32:135-40.
55. Koç K, Anik Y, Anik I, Cabuk B, Ceylan S. Chiari 1 malformation with syringomyelia: Correlation of phase-contrast cine MR imaging and outcome. Turk Neurosurg 2007;17:183-92.
56. Williams B. Cerebrospinal fluid pressure changes in response to coughing. Brain 1976;99:331-46.
57. Williams B. Experimental communicating syringomyelia in dogs after cisternal kaolin injection. Part 2. Pressure studies. J Neurol Sci 1980;48:109-22.
58. Williams B. Simultaneous cerebral and spinal fluid pressure recordings. 2. Cerebrospinal dissociation with lesions at the foramen magnum. Acta Neurochir (Wien) 1981;59:123-42.
59. Goel A. Instability and basilar invagination. J Craniovertebr Junction Spine 2012;3:1-2.
60. Goel A. Is syringomyelia pathology or a natural protective phenomenon? J Postgrad Med 2001;47:87-8.

61. Goel A, Shah A. Reversal of longstanding musculoskeletal changes in basilar invagination after surgical decompression and stabilization. J Neurosurg Spine 2009;10:220-7.
62. Goel A, Sharma P. Craniovertebral junction realignment for the treatment of basilar invagination with syringomyelia: Preliminary report of 12 cases. Neurol Med Chir (Tokyo) 2005;45:512-7.
63. Colby J, Dalton H, Whittenbury R. An improved assay for bacterial methane mono-oxygenase: Some properties of the enzyme from Methylomonas methanica. Biochem J 1975;151:459-62.
64. Goel A, Achawal S. The surgical treatment of Chiari malformation association with atlantoaxial dislocation. Br J Neurosurg 1995;9:67-72.
65. Goel A, Desai K. Surgery for syringomyelia: An analysis based on 163 surgical cases. Acta Neurochir (Wien) 2000;142:293-301.
66. Goel A, Desai KI, Muzumdar DP. Atlantoaxial fixation using plate and screw method: A report of 160 treated patients. Neurosurgery 2002;51:1351-6.
67. Goel A, Kulkarni AG, Sharma P. Reduction of fixed atlantoaxial dislocation in 24 cases: Technical note. J Neurosurg Spine 2005;2:505-9.
68. Goel A, Laheri V. Plate and screw fixation for atlanto-axial subluxation. Acta Neurochir (Wien) 1994;129:47-53.